Microwave MEMS-Based Voltage-Controlled Oscillators

Aleksander Dec, *Member, IEEE,* and Ken Suyama, *Senior Member, IEEE*

***Abstract*—A microwave voltage-controlled oscillator (VCO) based on coupled bonding wire inductors and microlectromechanical system (MEMS)-based variable capacitors for frequency tuning is demonstrated in this paper. The MEMS-based variable capacitors were fabricated in a standard polysilicon surface micromachining technology. The variable capacitors have a nominal capacitance of 1.4 pF and have a Q factor of 23 at 1 GHz and 14 at 2 GHz. The capacitance is variable from 1.4 to 1.9 pF as the tuning voltage is swept from 0 to 5 V. The VCO, fabricated in a 0.5-μm CMOS technology, was assembled in a ceramic package where MEMS and CMOS dice were bonded together. The oscillator operates at 2.4 GHz, achieves a phase noise of −122 dBc/Hz at 1-MHz offset from the carrier, and exhibits a tuning range of 3.4%.**

***Index Terms*—Tunable capacitors, voltage-controlled oscillators.**

I. Introduction

MANY MODERN wireless systems require high quality voltage-controlled oscillators (VCOs) that exhibit wide tuning range and low phase noise in the several gigahertz frequency range. Their tuning range must be large enough to cover the desired frequency span over process and temperature variations. The tunability is normally provided by a variable capacitor, which is often implemented as an external component because of the difficulty in realizing a high-Q factor on-chip variable capacitor. Achieving low phase noise translates to having a high-Q factor tank circuit and, hence, a high-Q factor inductor and variable capacitor [1]–[3]. Integrated VCOs normally rely on p–n junction varactors for frequency tuning [4]–[7]. In low phase-noise applications, however, the Q factor of an integrated p-n junction varactor is often inadequate and, hence, use of an alternative variable capacitor is often necessary.

Use of microelectromechanical systems (MEMS) for realization of microwave variable capacitors has recently been proposed [8], [9]. It has been shown that variable capacitors with a high-Q factor and wide tuning range can be implemented using either aluminum [8] or polysilicon [10] micromachining technologies, which makes these devices attractive for use in low phase-noise VCOs [11]–[14].

In addition to these desirable characteristics, a MEMS-based variable capacitor can handle large voltage swings, unlike a p-n junction varactor, where voltage swing must be limited to avoid placing the p-n junction in the forward bias region. Therefore, the phase noise of the oscillator can be improved by simply having a larger oscillation amplitude. Furthermore, MEMS-based variable capacitors do not respond to frequencies beyond their mechanical resonant frequencies. That is, the capacitance of these MEMS devices does not change with respect to microwave signals. Thus, these devices are not expected to produce harmonic distortion, which makes these devices suitable for microwave filter applications.

This paper presents a design of a 2.4-GHz CMOS *LC* VCO, which uses MEMS-based variable capacitors for frequency tuning [12]. After the design and characterization of the variable capacitors are discussed in Section II, the VCO circuit is described in Section III, and the experimental results are presented in Section IV. Effects of physical phenomena such as gravity, acceleration, vibration, and sound on the VCO behavior are discussed in Section V.

II. Variable Capacitor

The variable capacitor was designed in a multi-user MEMS processes (MUMPs) surface polysilicon micromachining technology [15]. The MUMPs process features three layers of polysilicon (poly0, poly1, and poly2) and one layer of gold, where gold can only be deposited on the top polysilicon layer (poly2). The poly0, poly1, poly2, and gold have thicknesses of 0.5, 2.0, 1.5, and 0.5 μm, respectively. The sheet resistance of poly0, poly1, poly2, and gold is 30 Ω/sq, 10 Ω/sq, 20 Ω/sq, and 0.06 Ω/sq, respectively. The sacrificial layer release consists of an HF etch of the oxide followed by a supercritical carbon dioxide drying process [15]. The supercritical drying process is used to ensure satisfactory device yield [16].

A. Device Operation

A functional diagram of the MEMS-based variable capacitor is shown in Fig. 1. The capacitor consists of two parallel plates where the top plate is supported by a spring, while the bottom plate is mechanically fixed. The capacitance C_D between the two plates is given by

$$C_D = \frac{\epsilon_D A}{x + d} \tag{1}$$

where ϵ_D is the dielectric constant, A is the area of the capacitor plates, d is the separation of the capacitor plates under zero-bias voltage, and x is the displacement of the suspended plate from its original position when a bias voltage across the plates is applied. The variable capacitor operates as follows: when a bias voltage is applied across the capacitor plates, an electrostatic force attracts the suspended plate toward the fixed plate until

Manuscript received July 16, 1999. This work was supported in part by the National Science Foundation under Grant CCR-98-03962.

The authors were with the Department of Electrical Engineering, Columbia University, New York, NY 10027 USA. They are now with Epoch Technologies, LLC, White Plains, NY, 10606 USA.

Publisher Item Identifier S 0018-9480(00)09546-6.

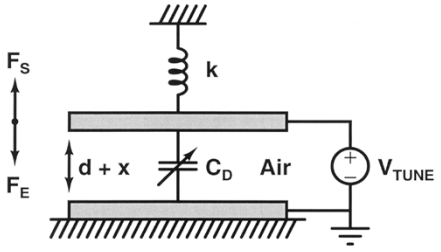

Fig. 1. Functional diagram of a MEMS-based variable capacitor.

an equilibrium between the spring and electrostatic forces is reached. The equilibrium between these two forces can be expressed as follows:

$$kx = \frac{1}{2}\frac{dC_D}{dx}V_{\mathrm{TUNE}}^2 \tag{2}$$

where k is the spring constant. By manipulating the equilibrium expression and solving for the displacement x, it can be shown that the solution exists only for displacements $0 > x > -d/3$. The maximum theoretical tuning range for this variable capacitor is then 1.5 : 1 [8], [10].

The dynamic behavior of the variable capacitor can be modeled by simply taking into account inertial force and friction as follows:

$$m\frac{d^2x}{dt^2} + r\frac{dx}{dt} + kx = \frac{1}{2}\frac{dC_D}{dx}V_{\mathrm{TUNE}}^2 \tag{3}$$

where m is the mass of the suspended plate and r represents the mechanical resistance or the presence of damping. It is of practical interest to investigate the frequency response of the variable capacitor to an excitation force F_{exc}. The transfer function can be obtained by setting the left-hand side of (3) to F_{exc} and by applying the Laplace transform to both sides as follows:

$$\frac{X}{F_{\mathrm{exc}}}(s) = \frac{1}{m}\cdot\left(\frac{1}{s^2 + \left(\dfrac{\omega_m}{Q_m}\right)s + \omega_m^2}\right) \tag{4}$$

where the mechanical resonant frequency ω_m and the mechanical quality factor Q_m are as follows:

$$\omega_m^2 = \frac{k}{m} \tag{5}$$

$$Q_m = \frac{\sqrt{km}}{r} \tag{6}$$

Note that the transfer function $X/F_{\mathrm{exc}}(s)$ has a low-pass response, which indicates that the variable capacitor is sensitive only to excitation forces whose frequencies fall within the mechanical resonance of the capacitor. High-frequency excitations are significantly attenuated.

B. Capacitor Design

Fig. 2(a) and (b) shows the top and cross-sectional views of the MEMS variable capacitor. The capacitor plates take an area of 230 μm $\times$ 230 μm and are separated by an air gap of 0.75 μm (after sacrificial layer release), which results in a nominal capacitance of 0.6 pF. The design goal is to achieve maximum theoretical tuning range of 1.5 : 1 within a 3.3-V control voltage, which can be achieved by using a suspension with a spring constant of 39 N/m. The suspended plate, which consists of poly2 and gold layers, has a mass of 0.8 μgram, while the mechanical resonant frequency is estimated at 35 kHz. To ensure the etch of the oxide between the capacitor plates, 141 holes were made in the capacitor plates. Holes were also made in the bottom capacitor plate to remove the oxide between the nitride and bottom capacitor plate and to reduce the bottom plate parasitic capacitance C_P. Gold is used where possible on the top capacitor plate and the suspension beams to maximize the Q factor.

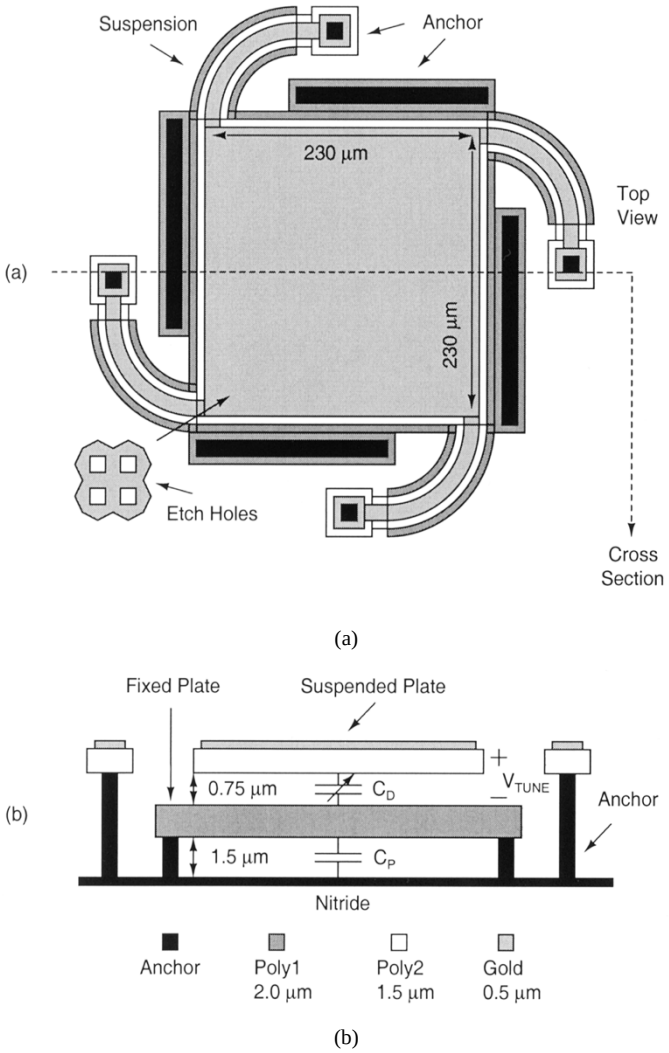

Fig. 2. (a) Top and (b) cross-sectional views of the variable capacitor (not to scale).

The suspension was designed with residual stress in mind. During the fabrication process, the polysilicon layers are deposited at high temperatures. As these layers cool down to room temperature, a certain amount of residual stress develops due to thermal expansion of polysilicon. In addition, the top plate of the capacitor consists of polysilicon and gold, two materials which have vastly different thermal expansion coefficients. Hence, the top capacitor plate tends to warp after the annealing and the sacrificial layer release. The suspensions fix the top plate in the xy-plane and, thus, a suspension, which can absorb some of the stress, is desirable. As is shown in Fig. 2(a), the suspension used

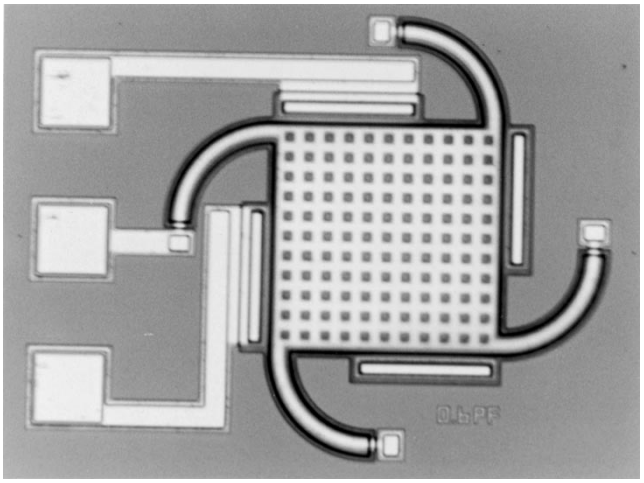

Fig. 3. Microphotograph of the variable capacitor.

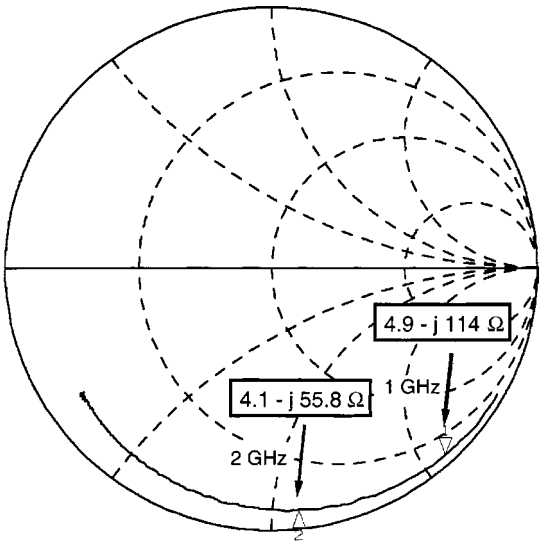

Fig. 4. S-parameters of the variable capacitor ($V_{\rm TUNE} = 0$ V

here allows horizontal rotational movement in the presence of stress in the top plate.

C. Measured Results

Fig. 3 shows the microphotograph of the MEMS variable capacitor. The variable capacitor was characterized using an HP8534D network analyzer, a Cascade probe station, and WinCal software. Fig. 4 shows the S-parameters of the variable capacitor. The variable capacitor has a nominal capacitance of 1.4 pF when $V_{\rm TUNE} = 0$ V and has a Q factor of 23 at 1 GHz and 14 at 2 GHz. The Q factor of the variable capacitor is mainly limited by the series resistance of the suspension [10]. Fig. 5 shows the tuning characteristics of the variable capacitor. As the bias voltage is swept from 0 to 5 V, the capacitance is tunable from 1.4 to 1.9 pF. The discrepancy between theoretical and measured capacitance is due to the residual stress [10]. Ten devices were fully characterized. The average nominal capacitance was 1.39 pF and the standard deviation was 0.03 pF. Although a larger number of devices must be characterized in order to obtain good statistics, these

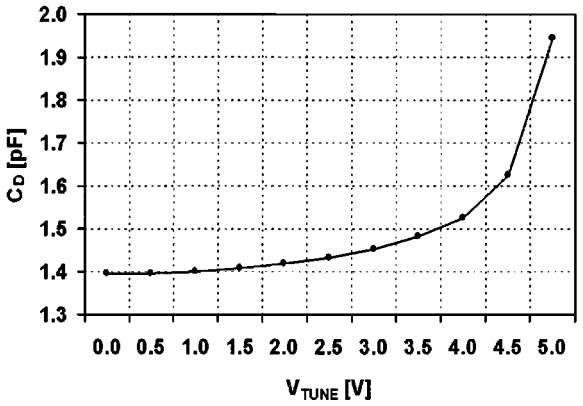

Fig. 5. Tuning characteristics of the variable capacitor.

TABLE I
SUMMARY OF VARIABLE CAPACITOR MEASUREMENTS

Nominal Capacitance	1.4 pF
Q-factor @ 1 GHz	23
Q-factor @ 2 GHz	14
Tuning Range	1.35:1
Tuning Voltage	5.0 V
Characterized Devices	10
Average Capacitance	1.39 pF
Standard Deviation	0.03 pF

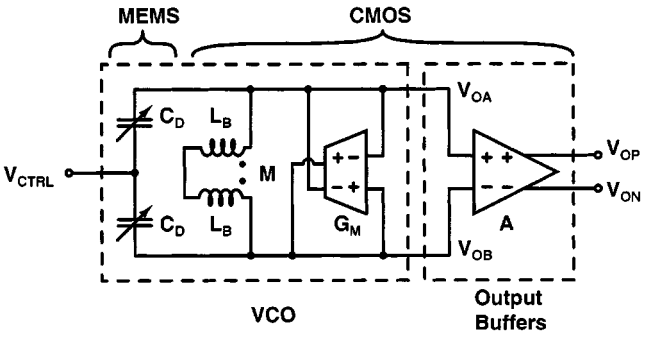

Fig. 6. Block diagram of the microwave MEMS-based VCO.

preliminary results indicate that these variable capacitors have relative matching of approximately 2%. Table I shows the summary of the measured results.

III. VCO CIRCUIT

The block diagram of the microwave MEMS-based VCO is shown in Fig. 6. The resonant circuit of the VCO consists of two variable capacitors (C_D) and bonding wire inductors (L_B) that are coupled together by mutual inductance (M). Bonding wire inductors are used because of their high-Q factors [17]. The negative conductance is realized using a cross-coupled transconductance amplifier (G_M). Output buffer (A) is used to isolate the resonant circuit from the load and to drive the measurement equipment.

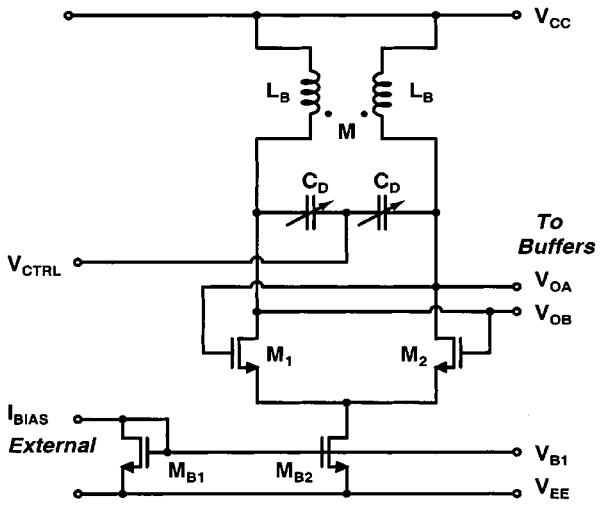

Fig. 7. VCO circuit.

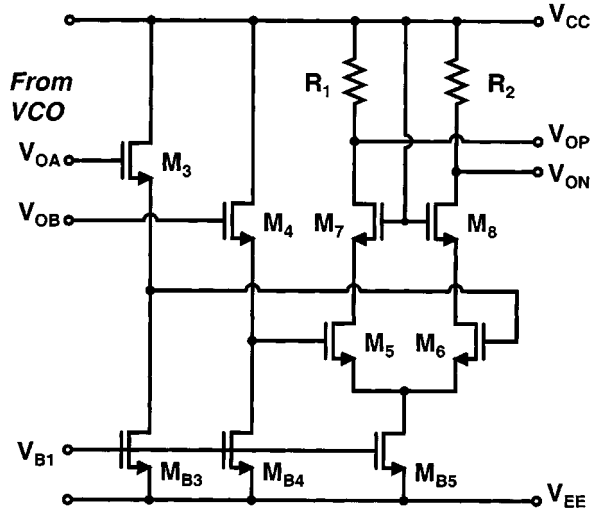

Fig. 8. Output buffers.

The circuit schematic of the VCO appears in Fig. 7. Differential pair ($M_1 - M_2$) realizes the transconductance amplifier (G_M). The bias current is provided by the current mirror ($M_{B1} - M_{B2}$) using externally supplied reference bias current ($I_{\rm BIAS}$). The oscillation frequency was arbitrarily chosen to be 2.4 GHz, which can be achieved by using 1.4-pF micromachined variable capacitors and 2.2-nH bonding wire inductors where the mutual inductance between the wires is 0.6 nH. The parasitic capacitance across the resonant circuit is approximately equal to the tunable capacitance. The inductors are realized using a 1-mil gold bonding wire, where each wire is 2.2-mm long and the two wires are separated by 0.5 mm. The coupled inductor has an estimated Q factor of 117 at 2.4 GHz. The variable capacitor has a Q factor of 11 at 2.4 GHz. The minimum required transconductance for oscillations to build up is 2.2 mS. However, the transconductance has been conservatively chosen to be approximately seven times larger than the minimum value necessary so that the circuit oscillates over process and temperature variations even if the MEMS-variable capacitor has a Q factor as low as five.

Fig. 8 shows the output buffers. Source followers ($M_3 - M_4$) buffer the oscillator output and drive the input of the cascoded differential pair amplifier ($M_5 - M_8$). On-chip 50-Ω resistors ($R_1 - R_2$) are used to accommodate the measurement equipment. Transistors ($M_{B3} - M_{B4}$) supply the bias current.

IV. Experimental Results

The variable capacitors were fabricated in a MUMPs polysilicon surface micromachining process, while the active circuits were implemented in an HP 0.5-μm CMOS technology. The VCO was assembled together by bonding the MUMPs and CMOS dice in a ceramic quad flat-pack package. The microphotograph of the packaged VCO appears in Fig. 9. The coupled bonding wire inductors are placed on the CMOS die (right-hand side), while variable capacitors are located on the MUMPs die (left-hand side). The bonding wires, which connect the MUMPs and CMOS dice, are approximately 0.8-mm long and separated by 150 μm. These bonding wires must be kept as short as possible to avoid parasitic oscillations. The active circuits occupy an area of 410 μm by 170 μm.

Fig. 10 shows the measurement setup. The external potentiometer ($R_{\rm EXT}$) is used to set the bias current. The two 100-pF capacitors provide dc blocking. The 4 : 1 transmission-line transformer performs differential to single-ended conversion. The HP 4352B VCO/PLL analyzer is used to analyze the output spectrum, phase-noise spectrum, and tuning characteristics of the VCO.

For the output spectrum and phase-noise spectrum measurements, the oscillation frequency of the VCO was set to 2.4 GHz by phase locking the VCO to a low phase-noise frequency reference using the internal narrow-band phase locked-loop (PLL) of the HP 4352B analyzer. Note that the HP 4352B analyzer automatically makes the bandwidth of the internal PLL sufficiently narrow so that for offset frequencies of interest only the VCO phase noise is measured. The output spectrum of the VCO is shown in Fig. 11. The VCO has an output level of -14 dBm.

The phase-noise spectrum of the VCO is shown in Fig. 12. At 100-kHz offset from the carrier, the phase noise is -93 dBc/Hz, while at 1-MHz offset from the carrier, the phase noise is -122 dBc/Hz. The phase noise of the VCO is caused not only by the electrical circuit noise, but also by the mechanical noise that is present in the variable capacitors. In theory, phase noise due to mechanical noise decays at a rate of -20 dB/dec for offset frequencies, well within the mechanical resonant frequency of the variable capacitor, and -60 dB/dec for offset frequencies far away from the mechanical resonant frequency [11]. For offset frequencies above 400 kHz, the phase noise of the VCO is dominated by the electrical circuit noise, which decays at -20 dB/dec. The close-in phase noise at offset frequencies below 400 kHz is dominated by the mechanical noise as well as $1/f$ noise of MOS devices.

Fig. 13 shows the tuning characteristics of the VCO. The oscillation frequency is tunable from 2400 to 2320 MHz, within a control voltage range of 6 V. Hence, the tuning range is 3.4%. Simulation results, however, indicate a wider tuning range based on the variable capacitor measurements. Further investigation

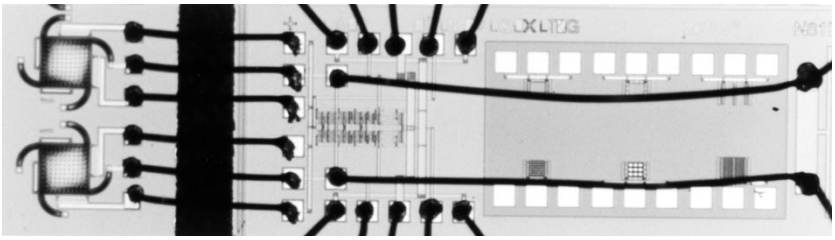

Fig. 9. Microphotograph of packaged VCO.

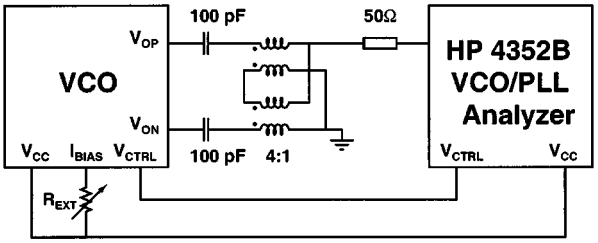

Fig. 10. Measurement setup.

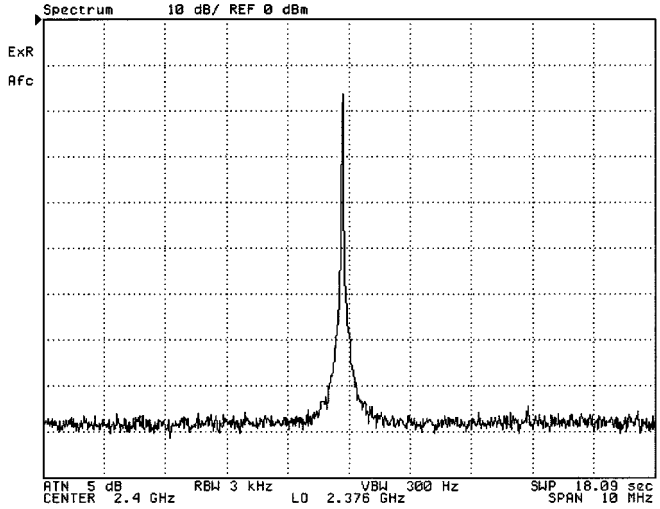

Fig. 11. Output spectrum.

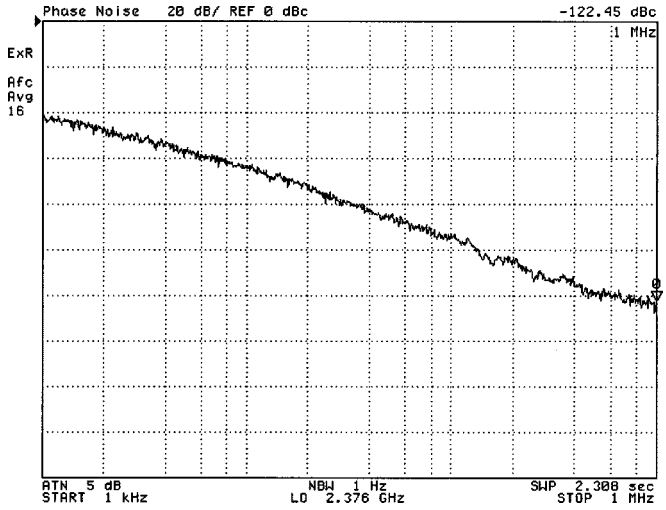

Fig. 12. Phase-noise spectrum.

reveals that the simulated oscillation frequency range can be achieved by applying larger tuning voltages, which effectively

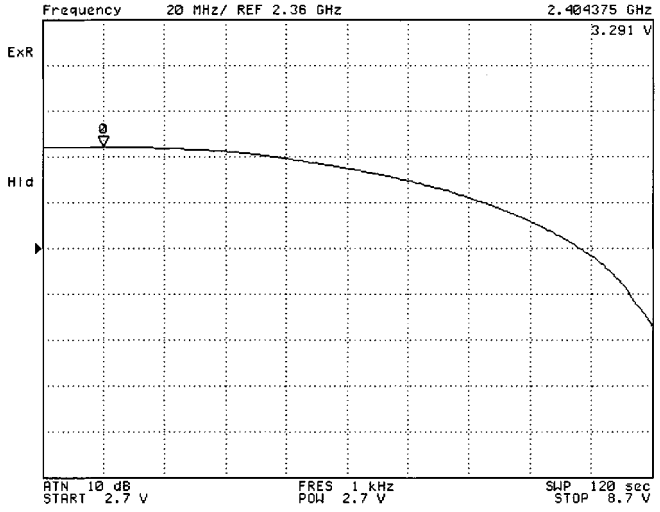

Fig. 13. Tuning characteristics.

TABLE II
SUMMARY OF VCO PERFORMANCE

Nominal Frequency	2.4 GHz
Tuning Range	3.4%
Phase Noise @ 100 kHz	-93 dBc/Hz
Phase Noise @ 1 MHz	-122 dBc/Hz
Output Level	-14 dBm
Power Supply	2.7 V
Supply Current (VCO Core)	5 mA
Supply Current (buffers)	15 mA

suggests an increase in the spring constant of the suspension, after bonding and packaging of the VCO. The oscillation frequency exhibits nonlinear relationship with respect to the tuning voltage and, consequently, the gain of the VCO is a function of the tuning voltage. An undesirable consequence of the nonconstant VCO gain, if the VCO is to be used in a frequency synthesizer, is the dependence of the settling time on the channel switching sequence. However, since the tuning voltage varies slowly, a nonlinear preprocessing circuit could, in principle, be designed as to make the oscillation frequency versus tuning voltage curve linear. The VCO consumes 20 mA of current, while operating from a 2.7-V power supply, where the VCO circuit and output buffers consume 5 and 15 mA, respectively. Measurement results are summarized in Table II.

V. Discussion

As with many electromechanical devices, influence of various physical phenomena such as gravity, acceleration, vibrations, and sound on MEMS-based variable capacitors and VCOs needs to be examined.

A. Effect of Gravity and Constant Acceleration

Since the suspended plate of the variable capacitor has a nonzero mass, its position changes with respect to gravity and acceleration. To examine the effect of constant acceleration on the variable capacitor, it is of interest to evaluate the sensitivity of the capacitance C_D to changes in the displacement δx as follows:

$$\frac{\delta C_D}{C_D} = -\frac{\delta x}{d+x}. \tag{7}$$

Similarly, the sensitivity of oscillation frequency to changes in the displacement δx can be shown to simplify to

$$\frac{\delta \omega_0}{\omega_0} = \frac{1}{2} \cdot \frac{1}{1+\gamma} \cdot \frac{\delta x}{d+x} \tag{8}$$

where γ is the ratio of parasitic to desired capacitance. The displacement of the suspended plate due to a constant acceleration G can be shown to be

$$\delta x = \frac{mG}{k}. \tag{9}$$

As an example, consider the variable capacitor design in Section II-B. Due to gravity, the distance between the capacitor plates would change by 0.2 nm and the 0.6-pF capacitance would change by approximately 0.027%, if the bias voltage is set to zero. The oscillation frequency would change by 0.007% (170 kHz for a 2.4-GHz oscillation frequency) if parasitic and desired capacitance are assumed to be equal. Similarly, in order to produce a 10% change in capacitance or a 2.5% change in oscillation frequency, an acceleration of 373 g would be required. In practice, the VCO would be employed in a PLL and, hence, the loop will adjust the control voltage so that the VCO oscillates at the desired reference frequency.

B. Effect of Vibrations and Sound

The effect of vibrations or dynamic acceleration on the variable capacitor can be evaluated in a similar fashion, as shown in the previous section, where the displacement due to dynamic acceleration $G(\omega)$ is now given by

$$|\delta x(\omega)| = \left| \frac{X}{F_{\text{exc}}}(\omega) \right| \cdot m \cdot |G(\omega)|. \tag{10}$$

Note that the displacement of the suspended capacitor plate varies mainly in response to low-frequency vibrations since the variable capacitor has a low-pass response $|X/F_{\text{exc}}(\omega)|$ with a cutoff frequency at the mechanical resonance. These low-frequency vibrations modulate the oscillation frequency of the VCO where the frequency deviation $\delta\omega_0$ is given by (8). As an example, a VCO based on the variable capacitor from Section II-B is considered where a vibration of 50 Hz with peak amplitude of 0.5 g is present. In the presence of the 0.5-g vibrations, the oscillation frequency deviates by approximately 0.0035%, a peak deviation of 85 kHz for a 2.4-GHz oscillation frequency. Note that the 50-Hz vibration falls well within the 35-kHz resonance of the variable capacitor.

Similarly, the effect of sound on the displacement of the suspended plate can be expressed as follows:

$$|\delta x(\omega)| = \left| \frac{X}{F_{\text{exc}}}(\omega) \right| \cdot |P_s(\omega)| \cdot A \tag{11}$$

where $P_s(\omega)$ is the pressure of sound. Given the variable capacitor from Section II-B, a 1-kHz tone 60 dB above the 20-μPa reference sound pressure (rms) would produce a displacement of 0.038 nm (rms) or an change in capacitance of 0.005% (rms). The 60-dB tone would result in a frequency deviation of 22 kHz (rms), if an oscillation frequency of 2.4 GHz is assumed. Naturally, the effect of sound is most severe if the variable capacitor is directly exposed to the external environment. However, the effect of sound on the variable capacitor can be minimized by packaging the device in a hermetically sealed package or even operating the device under vacuum. Moreover, the effect of these low-frequency excitations, in general, can be minimized by phase locking the VCO to a low-noise reference frequency and ensuring a wide-loop bandwidth of the PLL.

VI. Conclusion

A microwave MEMS-based VCO operating at 2.4 GHz was presented in this paper. The oscillator was fabricated in a 0.5-μm CMOS technology where the resonant circuit of the oscillator consists of coupled bonding wire inductors and MEMS-based variable capacitors. The variable capacitors, with a nominal capacitance of 1.4 pF and a Q factor of 23 at 1 GHz and 14 at 2 GHz, were fabricated in a standard polysilicon surface micromachining process. The capacitance is tunable from 1.4 to 1.9 pF as the bias voltage is swept from 0 to 5 V. The VCO was packaged in a ceramic package where MEMS and CMOS dice were bonded together. The VCO has a phase noise of -93 and -122 dBc/Hz at 100-kHz and 1-MHz offset from the 2.4-GHz carrier, respectively. The oscillation frequency is tunable by 3.4%. Future work includes the design of high-Q factor MEMS-based variable capacitors and the realization of fully monolithic microwave MEMS-based VCOs.

Acknowledgment

The authors would like to thank J. Schafer, Lucent Technologies, Holmdel, NJ, C. Petersen, Lucent Technologies, Murray Hill, NJ, D. Vallancourt, Lucent Technologies, Holmdel, NJ, and M. Banu, Lucent Technologies, Murray Hill, NJ, for their assistance in the packaging of the VCO and P. Caputo, Hewlett-Packard Company, Melville, NY, and M. Knox, Hewlett-Packard Company, Melville, NY, for providing the HP 4352B VCO/PLL analyzer.

References

[1] D. Leeson, "A simple model of feedback oscillator noise spectrum," *Proc. IEEE*, pp. 329–330, Feb. 1966.

[2] K. Kurokawa, "Some basic characteristics of broadband negative resistance oscillator circuits," *Bell Syst. Tech. J.*, pp. 1937–1955, July 1969.

[3] W. Robins, *Phase Noise in Signal Sources: Theory and Applications*. Stevenage, U.K.: Peregrinus, 1982, pp. 49–53.

[4] J. Craninckx and M. Steyaert, "A 1.8 GHz low-phase-noise spiral-LC CMOS VCO," in *VLSI Circuits Symp. Tech. Dig.*, June 1996, pp. 30–31.
[5] B. Razavi, "A 1.8-GHz CMOS voltage-controlled oscillator," in *IEEE ISSCC Tech. Dig.*, Feb. 1997, pp. 388–389.
[6] L. Dauphinee, M. Copeland, and P. Schvan, "A balanced 1.5 GHz voltage controlled oscillator with an integrated *LC* resonator," in *IEEE ISSCC Tech. Dig.*, Feb. 1997, pp. 390–391.
[7] M. Zannoth, B. Kolb, J. Fenk, and R. Weigel, "A fully integrated VCO at 2 GHz," in *IEEE ISSCC Tech. Dig.*, Feb. 1998, pp. 224–225.
[8] D. Young and B. Boser, "A micromachined variable capacitor for monolithic low-noise VCOs," in *IEEE Solid-State Sens. Actuator Workshop Dig.*, June 1996, pp. 86–89.
[9] A. Dec and K. Suyama, "Micromachined varactor with a wide tuning range," *Electron. Lett.*, vol. 33, no. 11, pp. 922–924, May 22, 1997.
[10] ——, "Micromachined electromechanically tunable capacitors and their applications to RF ICs," *IEEE Trans. Microwave Theory Tech.*, vol. 46, pp. 2587–2595, Dec. 1998.
[11] D. Young and B. Boser, "A micromachined based RF low noise voltage controlled oscillator," *IEEE Proc. CICC*, pp. 431–434, May 1997.
[12] A. Dec and K. Suyama, "A 1.9 GHz micromachined based low phase noise CMOS VCO," in *IEEE ISSCC Tech. Dig.*, Feb. 1999, pp. 80–81.
[13] ——, "A 2.4 GHz LC CMOS VCO with micromachined tunable capacitors for frequency tuning," in *IEEE MTT-S Int. Microwave Symp. Dig.*, June 1999, pp. 511–518.
[14] D. Young, J. Tham, and B. Boser, "A micromachine-based low phase-noise voltage controlled oscillator for wireless communications," in *Proc. Int. Solid-State Sens. Actuators Conf.*, June 1999, paper P4D4.1.
[15] D. Koester, R. Mahadevan, A. Shishkoff, and K. Markus, "Smart MUMP's design handbook including MUMP's introduction and design rules," *MEMS Technol. Applicat. Center*, pp. 1–8, July 1996.
[16] C. Dyck, J. Smith, S. Miller, E. Russick, and C. Adkins, "Supercritical carbon dioxide solvent extraction from surface micromachining micromechanical structures," *Proc. SPIE*, pp. 225–235, Oct. 1996.
[17] J. Craninckx and M. Steyaert, "A CMOS 1.8 GHz low phase noise voltage controlled oscillator with prescaler," in *IEEE ISSCC Tech. Dig.*, Feb. 1995, pp. 266–267.

Aleksander Dec (S'91–M'95) received the B.S., M.S., and Ph.D. degrees in electrical engineering from Columbia University, New York, NY, in 1993 and 1994, and 1998, respectively.

He was a Research Assistant at the Microelectronic Circuits and Systems Laboratory, Columbia University, from 1994 to 1998. He worked in the area of analog/RF integrated circuit design at Bell Laboratories, Murray Hill, NJ, in the summers of 1995, 1996, and 1997, respectively. He is currently with Epoch Technologies, LLC, White Plains, NY. His current research interests include analog/RF integrated-circuit design and application of MEMS devices to RF/microwave electronics.

Mr. Dec was a recipient of the 1995 Millman Outstanding Teaching Assistant Award.

Ken Suyama (S'81–M'82–SM'96) received the B.S. degree from the University of California at Davis, in 1980, and the M.S. and Ph.D. degrees from Columbia University, New York, NY, in 1982 and 1989, respectively.

He was an Associate Research Scientist from 1989 to 1992, an Assistant Professor from 1992 to 1994, and a Research Scientist from 1994 to 1998 in the Department of Electrical Engineering, Columbia University. He is currently with Epoch Technologies, LLC, White Plains, NY. His current research interests include analog/RF integrated circuits, mixed MEMS and integrated circuits, computer-aided design and analysis of integrated circuits, and chaotic neural networks.

Dr. Suyama is a member of the Board of Trustees and the President of the Catalyst Foundation. He was an associate editor of the IEEE TRANSACTIONS ON CIRCUITS AND SYSTEMS—PART II: ANALOG AND DIGITAL SIGNAL PROCESSING (1995–1997).